Second Law Analysis of Hydromagnetic Flow from a Stretching Rotating Disk: *DTM-Padé Simulation of Novel Nuclear MHD Propulsion Systems*

Mohammad Mehdi Rashidi[1], Osman Anwar Bég[*2], Navid Freidooni Mehr[1], Behnam Rostami[3]

Mechanical Engineering Department, Engineering Faculty of Bu-Ali Sina University, Hamedan, Iran

Director: Gort Engovation (Propulsion), 15 Southmere Avenue, Bradford, BD7 3NU, England, UK

Mechanical Engineering Department, Engineering Faculty of Bu-Ali Sina University, Hamedan, Iran

Young Researchers & Elites Club, Hamedan Branch, Islamic Azad University, Hamedan, Iran

[1]mm_rashidi@yahoo.com; [*2]gortoab@gmail.com; [3]nfreidoonimehr@yahoo.com; [4]behnam.rostami84@gmail.com

Abstract

In this paper, the second law analysis of hydromagnetic conducting flow due to a stretching rotating disk with heat transfer is investigated using a semi-analytical/numerical technique termed DTM-Padé simulation. The study has applications in rotating magneto-hydrodynamic (MHD) energy generators for new space systems and also thermal conversion mechanisms for nuclear propulsion space vehicles. The momentum and energy conservation equations are non-dimensionalized using appropriate transformations leading to a set of nonlinear, coupled, ordinary differential equations for momentum in the radial, azimuthal and normal directions and a temperature distribution equation. Using the appropriate velocity components and temperature field, the entropy generation equation is obtained. The effects of various parameters such as magnetic interaction parameter, rotation parameter, Eckert number, Brinkman number on the entropy generation and Bejan number are illustrated and described. The irreversibility mechanisms of the entropy generation for the emerging parameters are also investigated and suggestions for minimizing the entropy generation are proposed. The DTM-Padé results are verified with the numerical results and found to be in excellent agreement. The simulations also show the feasibility of using magnetic rotating disk drives in novel nuclear space propulsion engines.

Keywords

Second Law Analysis; Steady MHD Flow; Rotating Disk; Radial Stretching; Heat Transfer; DTM-Padé Simulation; Bejan Number; Swirling Flow; Nuclear Space Propulsion; Energy Generators

Introduction

The second law of thermodynamics is employed by engineers to obtain the optimal design of thermal systems via minimizing the irreversibility and entropy generation, which can improve the efficiency of industrial systems. Entropy generation involves thermodynamic irreversibilities, such as characteristics of convective heat transfer, heat transfer across finite temperature gradients, viscous dissipation effects and magnetic field effects which arise in modern aerospace heat transfer processes. The fluid flow and heat transfer processes are intrinsically irreversible, which leads to an increase entropy generation and useful energy destruction. Entropy generation has stimulated significant interest in recent years in aerospace thermal sciences. Erbay et al. used second law analysis to investigate computationally the entropy generation in a channel with a finite volume method and SIMPLE algorithm. Aïboud and Saouli applied second law thermodynamics to analyze the entropy generation in magneto-viscoelastic flow over a stretching surface. Al-Odat et al. simulated the effect of magnetic field on the entropy generation due to laminar forced convection over a horizontal flat plate with an implicit finite difference technique. Aïboud and Saouli further studied second law thermodynamics and viscoelastic magnetized flow from a stretching surface with double-diffusive convective heat and mass transfer, elaborating the influence of magnetic parameter, Reynolds number and Prandtl number on the entropy generation number. Sahin described the effect of the variable viscosity on the entropy generation in a laminar fluid flow, showing that the entropy generation due to viscous friction became dominant for low heat-flux terms. Ibáñez and Cuevas examined

entropy generation minimization of a hydromagnetic flow in a micro-channel. Makinde and Bég employed a perturbation expansion technique coupled with a special Hermite-Pade' approximations in the MAPLE program, to investigate volumetric entropy generation numbers, irreversibility distribution ratio and the Bejan number evolution in magneto-hydrodynamic channel flow in a plasma propulsion duct. Arikoglu et al. reported on the effect of slip in entropy generation from rotating disk in hydromagnetic flow with a differential transform method. Entropy generation analysis was applied to modeling and optimization of MHD induction devices by Salas et al.

Rotating Magneto-hydrodynamic (MHD) flows exploit magnetic fields which can induce currents in a movable conductive fluid. Liquid metals, plasmas and electrolytes are all important examples of MHD fluids. MHD flows also utilize a Lorentzian drag force which can be used to regulate a variety of flow regimes. Many applications exist for rotating hydromagnetic flows including propulsion systems, rotating MHD energy generators, smart spacecraft landing gear systems, hydrogen production with solar MHD plants, plasma fusion technology, nuclear thermal control systems, magneto-hydrodynamic chemical reactor processing and biomagnetic reactors. Many further applications of rotating hydromagnetic flows including swirling disk flows, flows from revolving cones in liquid metal stirring etc, are documented in the recent monograph by Bég et al.

In order to describe many physical systems with a mathematical model, nonlinear equations are used. Merical methods are frequently deployed to solve these complex systems of differential equations, which may be multi-degree and often strongly coupled. Although many powerful numerical techniques exist including finite element methods, network simulation, finite difference methods and CFD codes such as FLUENT, computational expense is always a problem. Therefore semi-numerical/analytical methods, such as the homotopy perturbation method (HPM), differential transform method (DTM) and homotopy analysis method (HAM) have found increasing popularity amongst aerospace fluid dynamics researchers. These techniques can successfully tackle nonlinear differential equations for a variety of boundary conditions, and therefore they hold significant promise in nuclear engineering sciences.

In this article, the second law analysis is employed to study the MHD fluid flow with heat transfer due to a stretching rotating disk. This problem was firstly studied by Turkyilmazoglu numerically, without considering entropy generation analysis. In this paper, these nonlinear swirling flow and heat conservation equations are solved via DTM-Padé simulation. As the second law analysis is more reliable than the first law analysis for many aerospace and nuclear engineering systems, entropy generation analysis is also included. In the current study, the effect of various thermophysical parameters, such as magnetic interaction parameter, rotation parameter, Eckert number, Prandtl number, Brinkman number and Reynolds number on velocity and temperature fields and also on the entropy generation and Bejan number are investigated in detail. The study has important applications in thermal optimization of novel MHD coupled nuclear space propulsion systems using rotating disks and hydromagnetics.

Mathematical Transport Model

The 3-dimensional steady magneto-hydrodynamic laminar boundary-layer flow of a Newtonian, electrically-conducting, viscous fluid from a rotating disk in the presence of an externally applied axially-directed uniform magnetic field is considered. This regime is often also termed hydromagnetic Von Karman swirling flow. The governing equations; the continuity, Navier-Stokes (momentum conservation), generalized Ohm's law and energy conservation equations can be presented, in the presence of Ohmic (Joule) heating and viscous dissipation, in vectorial form, as follows:

$$\nabla . \boldsymbol{u} = 0 \tag{1}$$

$$\rho(\boldsymbol{u} \cdot \nabla)\boldsymbol{u} = -\nabla P + \mu \nabla^2 \boldsymbol{u} + \boldsymbol{J} \times \boldsymbol{B} \tag{2}$$

$$\boldsymbol{J} = \sigma[\boldsymbol{E} + \boldsymbol{u} \times \boldsymbol{B}] \tag{3}$$

$$\rho c_p(\boldsymbol{u} \cdot \nabla)T = k\nabla^2 T + \mu \Phi + \boldsymbol{J}^2 / \sigma \tag{4}$$

where all parameters are defined in the nomenclature. The disc radius is much larger than the boundary layer thickness, so that edge effects can be neglected. The applied magnetic field is steady and sufficiently weak to neglect the induced magnetic field i.e. a low magnetic Reynolds number is assumed. This is a reasonable assumption for the flow of certain working fluids in novel nuclear-MHD propulsion systems and also in nuclear engineering liquid metals, e.g., liquid sodium. The physical regime is depicted in Fig. 1 with reference to non-rotating cylindrical polar coordinates where all parameters are defined in the nomenclature.

The disc radius is much larger than the boundary layer thickness, so that edge effects can be neglected. The applied magnetic field is steady and sufficiently weak to neglect the induced magnetic field i.e. a low magnetic Reynolds number is assumed. This is a reasonable assumption for the flow of certain working fluids in novel nuclear-MHD propulsion systems and also in nuclear engineering liquid metals, e.g., liquid sodium. The physical regime is depicted in Fig. 1 with reference to non-rotating cylindrical polar coordinates (r, θ, z).

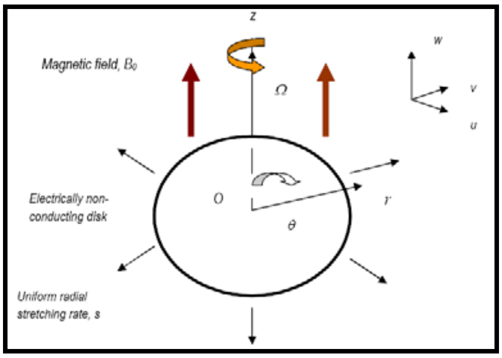

FIG. 1 3-D SWIRLING VON KARMAN MAGNETO-HYDRODYNAMIC FLOW REGIME AND COORDINATE SYSTEM

The disk rotates with a constant angular velocity (Ω) and also stretches with a constant rate (s) in the radial direction. The external uniform magnetic field ***B*** applies transverse to the disk plane i.e. in the z-direction and possesses a constant magnetic flux density B_0. Furthermore all thermophysical and fluid properties are assumed to be constant and radial and tangential electrical currents are neglected. The disk itself is electrically non-conducting, so that current density vanishes both at the disk surface and in the fluid regime. The penultimate and final terms on the right hand side of eqn. (9) designate the viscous heating and Joule heating contributions, respectively, and have been shown to be significant in propulsion applications. Following Turkyilmazoglu, the non-dimensional form for the mean flow velocities and temperature distribution are provided by Von Karman's classical transformations. With the aid of a dimensionless normal distance from the wall, $\eta = zR$, and an appropriate Reynolds number incorporating the disk stretching rate, $R = (s/\nu)^{1/2}$ we have:

$$(u, v, w, T) = \left(rsF(\eta), rsG(\eta), \frac{1}{R}H(\eta), T_\infty + (T_w - T_\infty)\theta(\eta) \right) \quad (5)$$

where the dimensionless functions F, G, H, and θ satisfy the following ordinary differential equations defining the radial, azimuthal, axial momentum conservation and energy conservation in the regime:

$$H' + 2F = 0 \quad (6)$$

$$F'' - F^2 + G^2 - HF' - MF = 0 \quad (7)$$

$$G'' - 2FG - HG' - MG = 0 \quad (8)$$

$$\theta'' - \Pr H\theta' + Ec\left(F'^2 + G'^2\right) + EcM\left(F^2 + G^2\right) = 0 \quad (9)$$

The boundary conditions at the stretching disk surface and in the free stream, are prescribed respectively, as:

$$\begin{aligned} &H = F - 1 = G - \omega = \theta - 1 = 0, \quad \text{at} \quad \eta = 0, \\ &F = G = \theta = 0 \quad \text{as} \quad \eta \to \infty, \end{aligned} \quad (10)$$

Here $\omega = \Omega/s$ denotes the "rotation strength parameter" expressing the ratio of disk swirl to disk radial stretch. The case of $\omega = 0$ corresponds to pure stretching of the disk without rotation. The nonlinear, coupled ODEs defined in eqns. (6)–(9) under boundary conditions (10) constitute a robust two-point boundary value problem, which may be readily solved with a variety of numerical or semi-numerical techniques. In the present study we implement a combination of the differential transform method (DTM) and Padé approximants, namely **DTM-Padé** simulation, which is described in due course.

Entropy Generation Analysis

The volumetric rate of local entropy generation, for the present hydromagnetic swirling heat transfer problem, in the presence of the axial symmetry, can be presented as follows:

$$\dot{S}'''_{gen} = \frac{k}{T_0^2}[\nabla T]^2 + \frac{\mu}{T_0}\Phi + \frac{1}{T_0}[(\boldsymbol{J} - \boldsymbol{QV})\cdot(\boldsymbol{E} + \boldsymbol{V} \times \boldsymbol{B})] \quad (11)$$

where:

$$[\nabla T]^2 = \left[\left(\frac{\partial T}{\partial r}\right)^2 + \left(\frac{1}{r}\frac{\partial T}{\partial \theta}\right)^2 + \left(\frac{\partial T}{\partial z}\right)^2 \right] \quad (12)$$

$$\begin{aligned} \Phi = 2&\left[\left(\frac{\partial u}{\partial r}\right)^2 + \frac{1}{r^2}\left(\frac{\partial v}{\partial \theta} + u\right)^2 + \left(\frac{\partial w}{\partial z}\right)^2 \right] \\ &+ \left(\frac{\partial v}{\partial z} + \frac{1}{r}\frac{\partial w}{\partial \theta}\right)^2 + \left(\frac{\partial w}{\partial r} + \frac{\partial u}{\partial z}\right)^2 + \left(\frac{1}{r}\frac{\partial u}{\partial \theta} + r\frac{\partial}{\partial z}\left(\frac{v}{r}\right)\right)^2 \end{aligned} \quad (13)$$

$$\boldsymbol{J} = \sigma[\boldsymbol{E} + \boldsymbol{u} \times \boldsymbol{B}] \quad (14)$$

It is assumed that electric force per unit charge is negligible compared with ***V***×***B*** in Eqs. (11) and (14) and furthermore that electric current is much greater than ***QV***. With these assumptions, Eq. (11) can be

shown to take the form:

$$\dot{S}'''_{gen} = \frac{k}{T_0^2}\left(\frac{\partial T}{\partial z}\right)^2 + \frac{\mu}{T_0}\left\{\begin{matrix} 2\left[\left(\frac{\partial u}{\partial r}\right)^2 + \frac{1}{r^2}u^2 + \left(\frac{\partial w}{\partial z}\right)^2\right] + \\ \left(\frac{\partial v}{\partial z}\right)^2 + \left(\frac{\partial u}{\partial z}\right)^2 + \left(r\frac{\partial}{\partial z}\left(\frac{v}{r}\right)\right)^2 \end{matrix}\right\} + \frac{\sigma B_0^2}{T_0}\left(u^2+v^2\right) \quad (15)$$

The right hand side of the above entropy generation equation consists of three parts. The first term is the local entropy generation due to heat transfer irreversibility. The second larger part refers to the fluid friction irreversibility. The final part denotes magnetic field effects. The dimensionless form of the entropy generation rate, termed entropy generation number, defines the ratio between the actual entropy generation rate $\dot{S}'''_{gen}$ and the characteristic entropy generation rate $\dot{S}'''_0$. By using the Von Karman transformation parameters, as defined in Eq. (5), the entropy generation number (N_G) becomes, for the present problem:

$$N_G = \alpha\theta'(\eta)^2 + \frac{4Br}{\mathrm{Re}}F(\eta)^2 + \frac{2Ec}{\mathrm{Re}}H'(\eta)^2 + Br\left(F'(\eta)^2 + G'(\eta)^2\right) + BrM\left(F(\eta)^2 + G(\eta)^2\right) \quad (16)$$

Inspection of Eq. (16), indicates that with increasing value of α, the effect of heat transfer irreversibility increases. As the Brinkman number and Eckert number increase or the Reynolds number decreases, the entropy generation due to fluid friction irreversibility increases. Irreversibility mechanism domination is an important aspect of entropy generation analysis since the entropy generation number does not provide any information regarding this. The Bejan number and the irreversibility distribution ratio are introduced to overcome this shortcoming. The Bejan number (Be) embodies the ratio of entropy generation which is caused through heat transfer to the total entropy generation. The irreversibility distribution ratio (φ) expresses the ratio between entropy generation due to fluid friction and joule dissipation in heat transfer. These two parameters, for the present swirling magnetohydrodynamic thermal problem can be expressed as:

$$Be = \frac{\alpha\theta'(\eta)^2}{\alpha\theta'(\eta)^2 + \frac{4Br}{\mathrm{Re}}F(\eta)^2 + \frac{2Ec}{\mathrm{Re}}H'(\eta)^2 + Br\left(F'(\eta)^2 + G'(\eta)^2\right) + BrM\left(F(\eta)^2 + G(\eta)^2\right)} \quad (17)$$

$$\phi = \frac{\frac{4Br}{\mathrm{Re}}F(\eta)^2 + \frac{2Ec}{\mathrm{Re}}H'(\eta)^2 + Br\left(F'(\eta)^2 + G'(\eta)^2\right) + BrM\left(F(\eta)^2 + G(\eta)^2\right)}{\alpha\theta'(\eta)^2} \quad (18)$$

As illustrated by the definitions of the above dimensionless parameters, the behavior of the Bejan number and irreversibility distribution ratio are almost the same. Thus we only examine the Bejan number effects in this article. The Bejan number falls in the range, $0 < Be < 1$. When $Be = 0$, fluid friction irreversibility dominates. For $Be = 0.5$, heat transfer and fluid friction irreversibility effects are the same. For $Be = 1$, the irreversibility mechanism is dominated by heat transfer effects.

DTM- Padé Simulation

In the current article, DTM is employed in conjunction with Padé approximants to solve the governing equations (6) to (9), under boundary conditions (10). Zhou was the first one who developed DTM for electrical circuit modeling. The principal attraction of this technique is that it can be applied directly to nonlinear differential equations without requiring discretization and linearization, a strong advantage over purely numerical methods such as finite elements and finite differences. DTM also does not require any perturbation parameters and this offers a great advantage over asymptotic and perturbation expansion techniques. This method has been successfully implemented in a diverse array of including nanofluid, hypersonic, swirl flow and geothermic flow. In order to solve highly nonlinear differential equation systems, arising frequently in nuclear engineering fluid dynamics, it is pertinent to combine DTM with Padé approximations and use DTM-Padé simulation. This method effectively increases the convergence of DTM. Further details are given in ref. Numerous mathematical techniques exist to increase the convergence radius of a given series. The Padé approximant is a rational fraction. Details of

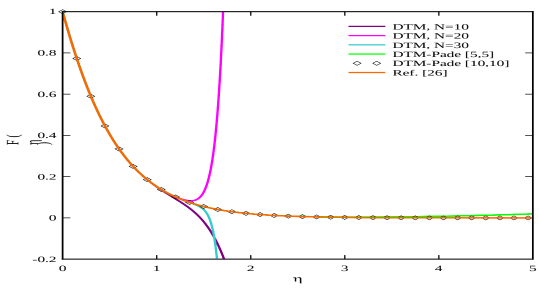

FIG. 2 RADIAL VELOCITY COMPONENT, $F(\eta)$ OBTAINED BY DTM FOR DIFFERENT N AND ORDERS OF DTM-PADÉ IN COMPARISON WITH REF. [26] FOR $\omega = 1, M = 2$.

such approximants are provided in Baker and Graves-Morris. The approximants are generated numerically using *MATHEMATICA* software. Stability, consistency and convergence are successfully achieved by DTM-Padé simulation. DTM alone diverges (figure 2).

Results and Discussion

To verify the validity of the present computations, results have been benchmarked with the non-entropy study of Turkyilmazoglu. Excellent correlation between the semi-numerical/analytical results obtained by DTM-Padé (Padé approximant of order) and the Chebsyhev spectral collocation numerical computations of Turkyilmazoglu is achieved, as observed in Fig 3. Confidence in the present DTM-Padé solutions is therefore high. We note that the case of equal rotational strength and disk stretching corresponds to $\omega = 1$. The cases of $\omega = 0$ i.e. pure stretching of the disk without rotation, and $\omega \to \infty$ i.e. pure rotation of the disk without stretching are extreme scenarios and not considered in the present study.

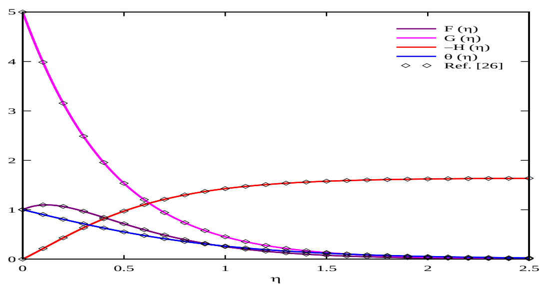

FIG. 3 RADIAL, AZIMUTHAL AND AXIAL VELOCITY FUNCTIONS AND TEMPERATURE FUNCTION OBTAINED BY DTM-PADÉ (PADÉ APPROXIMANTS [10, 10]) IN COMPARISON WITH REF. [26] WITH $\Pr = Ec = 1$, $M = 2$ AND $\omega = 3$

Figures 4-7 present the velocity contours in all directions. As the radial coordinate increases, the primitive radial (u) and azimuthal (v) velocity components clearly increase. These velocity components are maximized near the surface of the disk i.e. at low values of axial coordinate (bottom right hand corner of both Figs. 4 and 5). The velocity vectors are shown in Fig. 7, in order to have a better grasp of the fluid flow. In both cases although ω has been prescribed as 1, the disk stretch rate is very high at 10. Conversely in Fig. 6 we observe that axial velocity component is maximized near the disk surface for all values of radial coordinate (lower red band). The axial velocity clearly decays as we depart from the surface and is minimized at greater distances from the disk $(z \sim 0.4)$. Figure 7 distinctly shows the convergence of velocity vectors (u, w) towards the bottom right hand corner of the plot i.e. fluid is clearly drawn in a fan like mechanism outwards along the radial coordinate and in the negative axial direction. This pattern typifies Von Karman swirling flow.

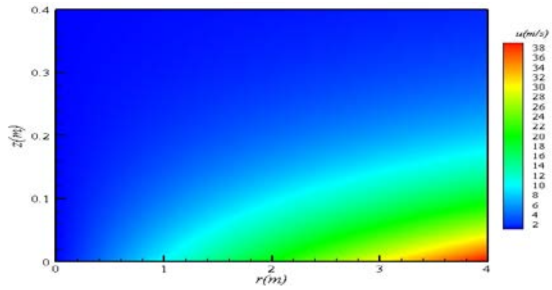

FIG. 4 RADIAL VELOCITY CONTOURS WITH $M = \omega = 1$, $\Pr = Ec = 2$, $\nu = 9 \times 10^{-6}$ AND $s = 10$.

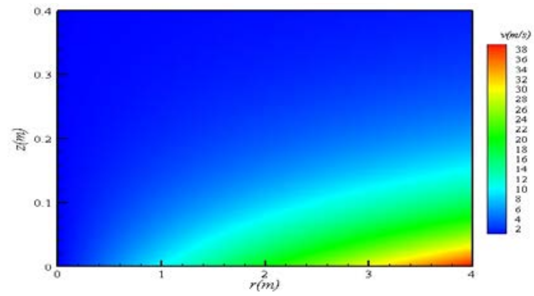

FIG. 5 AZIMUTHAL VELOCITY CONTOURS WITH $M = \omega = 1$, $\Pr = Ec = 2$, $\nu = 9 \times 10^{-6}$ AND $s = 10$.

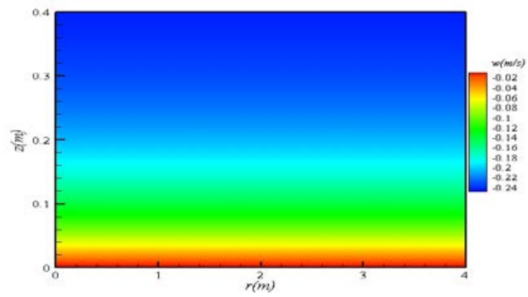

FIG. 5 AXIAL VELOCITY CONTOURS WITH $M = \omega = 1$, $\Pr = Ec = 2$, $\nu = 9 \times 10^{-6}$ AND $s = 10$.

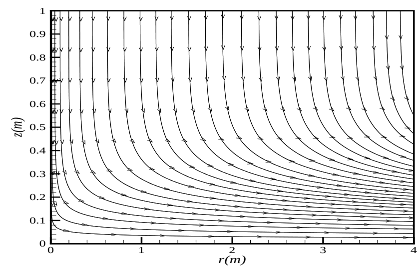

FIG. 7 VECTOR VARIABLES OF u AND w WITH $M = \omega = 1$, $\Pr = Ec = 2$, $\nu = 9 \times 10^{-6}$ AND $s = 10$.

Figures 8-13 illustrate the influence of the emerging thermophysical parameters on entropy generation number, and Bejan number distributions, with radial

coordinate. In each of these graphs, dimensionless temperature difference is set to unity.

The entropy generation number and Bejan number variation with changing magnetic interaction parameter are presented in Figs. 8 and 9. As the magnetic interaction parameter increases, the amount of entropy generation increases considerably (it is minimized in the absence of a magnetic field, $M = 0$). This implies that in order to control the entropy which is generated from swirling flow on the disk surface, the value of magnetic interaction parameter should be reduced, an issue of interest in nuclear-MHD rotating disk propulsion. The fluid friction irreversibility is dominated mechanism of irreversibility, and is distant from of the disk surface for small values of magnetic interaction parameter. As the magnetic interaction parameter is elevated, the heat transfer mechanism dominates irreversibility. It should also be mentioned that a minimum point arises for Bejan number near the disk surface for any value of magnetic interaction parameter. At large values of M the Bejan number escalates and after ascending very sharply from the disk surface converges asymptotically to the maximum allowable value of unity, a trend sustained into the free stream. In essence when entropy generation is maximized, the Bejan number is minimized and vice versa in the swirling flow regime.

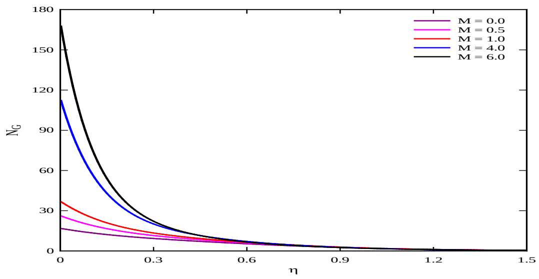

FIG. 8 THE VARIATION OF ENTROPY GENERATION NUMBER, N_G WITH MAGNETIC INTERACTION PARAMETER FOR $\Pr = Ec = 2,\ Br = 4,\ \mathrm{Re} = 8$ AND $\omega = 1$.

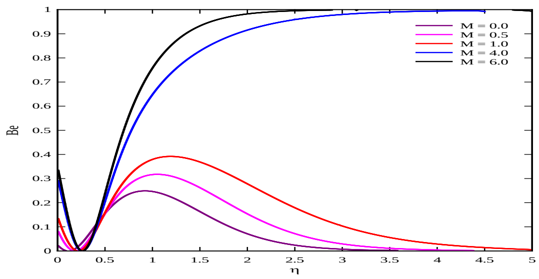

Fig. 9 THE VARIATION OF BEJAN NUMBER, Be WITH MAGNETIC INTERACTION PARAMETER FOR $\Pr = Ec = 2,\ Br = 4,\ \mathrm{Re} = 8$ AND $\omega = 1$.

Figures 10, 11 illustrate the effect of rotation strength parameter on the entropy generation and Bejan number distributions with radial coordinate. An increase in ω generates a similar but more pronounced response to that of increasing magnetic interaction parameter i.e. it causes a considerable increase in N_G near the disk surface, leading to a maximum entropy generation value always at the disk surface itself. Further from the disk N_G profiles decay sharply to vanish in the free stream. The Bejan number is generally minimized closer to the disk and maximized further from the disk, in direct contrast to the entropy generation number. In all cases, the lowest value of Bejan number arises in the same vicinity as the maximum value of entropy generation number i.e. near the disk surface. For larger values of rotation strength parameter Bejan number achieves the asymptotic profile sooner. In the asymptotic state where the profiles all converge on unity in the free stream, the heat transfer irreversibility is dominant.

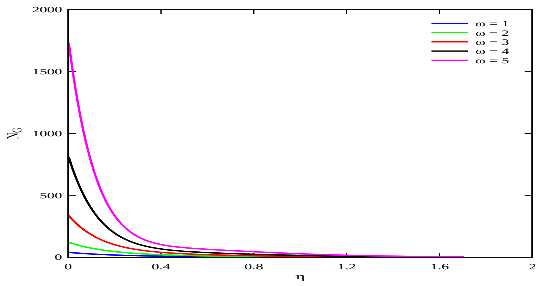

FIG. 10 THE VARIATION OF ENTROPY GENERATION NUMBER, N_G WITH ROTATION STRENGTH PARAMETER FOR $\Pr = Ec = 1,\ M = 2,\ Br = 3$ AND $\mathrm{Re} = 6$.

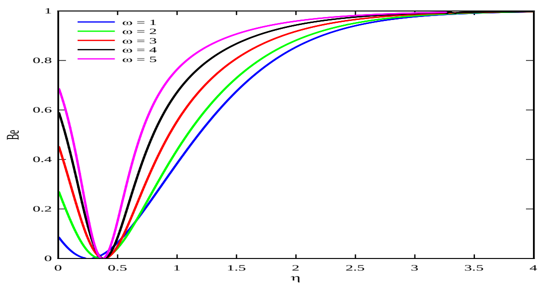

FIG. 11 THE VARIATION OF BEJAN NUMBER, Be WITH ROTATION STRENGTH PARAMETER FOR $\Pr = Ec = 1,\ M = 2,\ Br = 3$ AND $\mathrm{Re} = 6$.

Figures 12 and 13 depict the response of the entropy numbers to Eckert number. Increasing Eckert number significantly increases the entropy generation number, N_G increases, as the Eckert number increases. It should also be noted that at a certain distance from the disk surface $(\eta \cong 0.45)$, the amount of generated entropy converges on the same value for all Eckert numbers. The influence of Eckert number on the Bejan

number (Be) profiles is similar to those induced by the rotational strength parameter. Brinkman number, $Br = \mu s^2 r^2 / k\Delta T$ represents the ratio of direct heat conduction from the disk surface to the viscous heat generated by shear in the boundary layer. It is distinct from Eckert number which symbolizes the kinetic energy of flow to the boundary layer enthalpy difference. It is in fact more appropriate for industrial flows, whereas Eckert number often arises in high-speed aerodynamic flows. Both parameters are quantifications of viscous dissipation effects. Bejan number decays from a high value at the disk surface to a minimum near the disk surface and then ascends rapidly to converge on unity in the free stream. A rise in Ec clearly enhances Bejan number. In all cases we have considered positive Ec values i.e. heat is transferred from the disk surface to the fluid by convection currents. Further from the disk surface heat transfer irreversibility dominates. For large values of Prandtl number, the fluid friction irreversibility dominates compared with heat transfer. Bejan number is clearly a maximum when entropy generation number is a minimum.

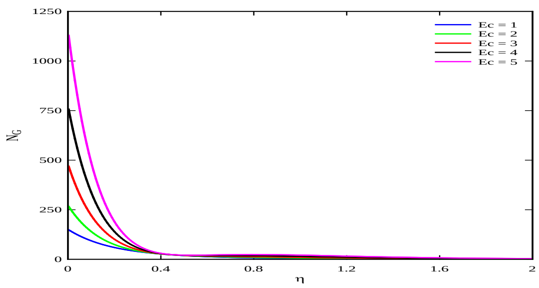

FIG. 12 THE VARIATION OF ENTROPY GENERATION NUMBER, N_G WITH ECKERT (VISCOUS HEATING) NUMBER FOR $\Pr = 1,\ \omega = M = 2,\ Br = 4$ AND $\mathrm{Re} = 6$.

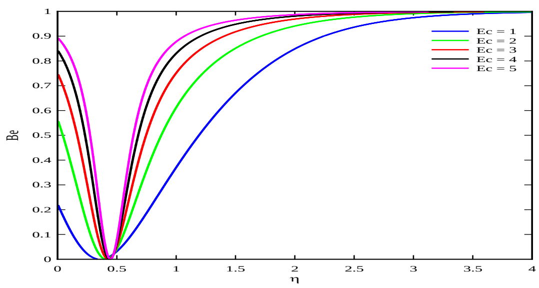

FIG. 13 THE VARIATION OF BEJAN NUMBER, Be WITH ECKERT (VISCOUS HEATING) NUMBER FOR $\Pr = 1,\ \omega = M = 2,\ Br = 4$ AND $\mathrm{Re} = 6$.

We further note that the correct trends for entropy generation number and Bejan number have been achieved by DTM-Padé simulation and have been concurred with the observations documented in other studies, for example Aïboud and Saouli and Arikoglu et al., the latter considering Von Karman swirling hydromagnetic flow with slip effects. As the Brinkman number increases, the effect of fluid friction irreversibility is amplified on the disk surface. Further from the disk surface, the effect of heat transfer irreversibility becomes larger as the Brinkman number decreases. For high Br, the effects of heat transfer and fluid friction irreversibilities are almost equal. Effectively, the present semi-numerical computations testify that the contribution of Brinkman number, as originally proposed and elucidated by Bejan and further implemented in hydromagnetic heat transfer by Makinde and Bég, is therefore of significance in second law thermodynamic analysis, and plays an important potential role in nuclear MHD spacecraft engine thermodynamic optimization.

Conclusions

In the current investigation, second law thermodynamic analysis has been utilized to obtain the entropy generation equations for swirling Von Karman hydromagnetic flow with heat transfer from a stretching rotating disk. A semi-numerical technique amalgamating the differential transform method (DTM) and Padé approximants i.e. DTM-Padé simulation, has also been applied to determine solutions for the transformed momentum and energy conservation equations describing the swirling fluid dynamics, under appropriate boundary conditions. The nonlinear coupled multi-degree boundary value problem has been very efficiently solved with benchmarking to numerical shooting quadrature, demonstrating excellent correlation between both methods. The velocity contours in all directions and velocity vectors have been visualized to illustrate the actual dynamics of the flow in primitive coordinates. Furthermore the influence of Brinkman number on entropy generation number and Bejan number, have also been presented and analyzed. The powerful contributions of disk swirl and disk stretch (investigated via the rotational strength parameter), magnetic field retardation and viscous heating on the flow variables have clearly been identified in the computations. The fundamental objective of second law thermodynamics analysis has been also achieved, namely, minimization of entropy in the swirling disk flow regime. The present computations have provided some further insight into the thermodynamics and fluid mechanics of proposed rotating disk MHD systems coupled with nuclear space propulsion

engines, although these require further evaluation, in particular for transient and magnetic induction effects, aspects which are under consideration by the authors. DTM-Padé simulation holds excellent potential in analyzing such aerospace problems.

REFERENCES

Abu-Nada, E. "Entropy Generation due to Heat and Fluid Flow in Backward Facing Step Flow with Various Expansion Ratios" International Journal of Exergy 3 (2006): 419-35.

Aïboud, S., and S. Saouli. "Entropy Analysis For Viscoelastic Magnetohydrodynamic Flow over a Stretching Surface" International Journal of Non-Linear Mechanics 45 (2010): 482-9.

Aïboud, S., and S. Saouli. "Second Law Analysis of Viscoelastic Fluid over a Stretching Sheet Subject to a Transverse Magnetic Field with Heat and Mass Transfer" Entropy 12 (2010): 1867-84.

Al-Odat, M., Damseh, R., and M.A. Al-Nimr. "Effect of Magnetic Field on Entropy Generation due to Laminar Forced Convection Past a Horizontal Flat Plate" Entropy 6 (2004): 293-303.

Anghaie, S. "Prospect of nuclear power MHD conversion, Proceedings of 6th International Symposium Propulsion for Space Transportation of the 21st Century, Versailes, France, May (2002): 14-17.

Anwar Bég, O., Ghosh, S.K., Ahmed, S., and T.A. Bég. "Mathematical Modelling of Oscillatory Magneto-Convection of a Couple Stress Biofluid in an Inclined Rotating Channel" Journal of Mechanics in Medicine and Biology 12 (2012) 10.1142/S0219519411004654.

Anwar Bég, O., Ghosh, S.K., and Anwar Bég, T., Applied Magneto-Fluid Dynamics: Modelling and Computation, Lambert Academic Publishing, Germany, 2011.

Anwar Bég, O., Ghosh, S.K., and M. Narahari. "Mathematical Modelling of Oscillatory MHD Couette Flow in a Rotating Highly Permeable Medium Permeated by an Oblique Magnetic Field" Chemical Engineering Communications 198 (2011): 235-54.

Anwar Bég, O., Makinde, O.D., Zueco, J., and S.K. Ghosh. "Hydromagnetic Viscous Flow in a Rotating Annular High-Porosity Medium with Nonlinear Forchheimer Drag Effects: Numerical Study" World Journal of Modelling and Simulation 8 (2012): 83-95.

Anwar Bég, O., Prasad, V.R., Vasu, B., Bhaskar Reddy, N., Li, Q., and R. Bhargava. "Free Convection Heat and Mass Transfer from an Isothermal Sphere to a Micropolar Regime with Soret/Dufour Effects" International Journal of Heat and Mass Transfer 54 (2011): 9-18.

Anwar Bég, O., Rashidi, M.M., Aziz, A., and M. Keimanesh. "Differential transform study of hypersonic laminar boundary layer flow and heat transfer over slender axisymmetric bodies of revolution" International Journal of Applied Mathematics and Mechanics 8 (2012): 83-108.

Anwar Bég, O., Sim, L., Zueco, J., and R. Bhargava. "Numerical Study of Magnetohydrodynamic Viscous Plasma Flow in Rotating Porous Media with Hall Currents and Inclined Magnetic Field Influence" Communications in Nonlinear Science and Numerical Simulation 15 (2010): 345-59.

Anwar Bég, O., Zueco, J., and L.M. López-Ochoa. "Network numerical Analysis af Optically-Thick Hydromagnetic Slip Flow From a Porous Spinning Disk with Radiation Flux, Variable Thermophysical Properties and Surface Injection Effects" Chemical Engineering Communications 198 (2011): 360-84.

Arikoglu, A., Ozkol, I., and G. Komurgoz. "Effect of Slip on Entropy Generation in a Single Rotating Disk in MHD Flow" Applied Energy 85 (2008): 1225-36.

Baker, G.A., and P.R. Graves-Morris, Padé Approximants: Basic Theory, Addison-Wesley, USA, 1981.

Bejan, Adrian. Entropy generation through heat and fluid flow: Wiley, New York, 1982.

Bejan, Adrian. Entropy generation minimization: the method of thermodynamic optimization of finite-size systems and finite-time processes: CRC Press, Florida, 1996.

Bejan, A. "A Study of Entropy Generation in Fundamental Convective Heat Transfer", ASME Journal of Heat Transfer 101 (1979): 718-25.

Daud, H.A., Li, Q., Anwar Bég, O., and S.A.A. AbdulGhani. "Numerical Investigations of Wall-Bounded Turbulence" Proceedings of the Institution of Mechanical Engineers, Part C: Journal of Mechanical Engineering Science 225 (2011): 1163-74.

Erbay, L., Ercan, M., Sülüs, B., and M. Yalçÿn. "Entropy

Generation During Fluid Flow Between Two Parallel Plates with Moving Bottom Plate" Entropy 5 (2003): 506-18.

Fang, T. "Flow over a stretchable disk, Physics of Fluids" 19 (2007): 128105-10.

Ghosh, S.K., Anwar Bég, O., Zueco J, and V.R. Prasad. "Transient Hydromagnetic Flow in a Rotating Channel Permeated by an Inclined Magnetic Field With Magnetic Induction and Maxwell Displacement Current Effects" ZAMP: Journal of Applied Mathematics and Physics 61 (2010): 147-69.

Hayat, T., Naza, R., Asghar, S., and S. Mesloub. "Soret–Dufour Effects on Three-Dimensional Flow of Third Grade Fluid" Nuclear Engineering and Design 243 (2012): 1- 14.

Ibáñez, G., and S. Cuevas. "Entropy Generation Minimization of a MHD (Magnetohydrodynamic) Flow in a Micro-Channel" Energy 35 (2010): 4149-55.

Intani, P., Sasaki, T., Kikuchi, T., and N. Harada. "Analysis of Disk AC MHD Generator Performance by Finite Element Method" Journal of Plasma Fusion Research 9 (2010): 580-5.

Kabakov, V.I., and Y.I. Yantovsky. "Solar Pond Magnetohydrodynamic Generator for Hydrogen Production" International Journal of Hydrogen Energy 18 (1993): 19-23.

Lee, C.C., Jones, O.C., and M. Becker. "Thermofluid-Neutronic Stability of the Rotating, Fluidized Bed, Space-Power Reactor" Nuclear Engineering and Design 139 (1993): 17-30.

Makinde, O.D., and O. Anwar Bég. "On Inherent Irreversibility in a Reactive Hydromagnetic Channel Flow" Journl of Thermal Science 19 (2010): 1-8.

Pop, I, and V.M. Soundalgekar. "The Hall Effect on an Unsteady Flow due to a Rotating Infinite Disc" Nuclear Engineering and Design 44 (1977): 309-14.

Prasad, V.R., Vasu, B., Anwar Bég, O., and R. Parshad. "Unsteady Free Convection Heat and Mass Transfer in a Walters-B Viscoelastic Flow Past a Semi-Infinite Vertical Plate: a Numerical Study" Thermal Science 15 (2011): 291-305.

Rashidi, M.M., Anwar Bég, O., and N. Rahimzadeh. "A generalized DTM for combined free and forced convection flow about inclined surfaces in porous media" Chemical Engineering Communications 199 (2012): 257-82.

Rashidi, M.M., Anwar Bég, O., Asadi, M., and M.T. Rastegari. "DTM-Padé modeling of natural convective boundary layer flow of a nanofluid past a vertical surface" International Journal of Thermal and Environmental 4 (2012): 13-24.

Rashidi, M.M., Erfani, E., Anwar Bég, O., and R.S. Gorla. "Modified Differential Transform Method (DTM) simulation of hydromagnetic multi-physical flow phenomena from a rotating disk" World Journal of Mechanics 5 (2011): 217-30.

Rashidi, M.M., Keimanesh, M., Anwar Bég, O., and T.K. Hung. "MHD Bio-Rheological Transport Phenomena in a Porous Medium: a Simulation of Magnetic Blood Flow Control and Filtration", International Journal for Numerical Methods in Biomedical Engineering 27 (2011): 805-21.

Rawat, S., Bhargava, R., and O. Anwar Bég. "Transient Magneto-Micropolar Free Convection Heat and Mass Transfer Through a Non-Darcy Porous Medium Channel with Variable Thermal Conductivity and Heat Source Effects" Proceedings of the Institution of Mechanical Engineers, Part C: Journal of Mechanical Engineering Science 223 (2009): 2341-55.

Sahin, A. "The Effect of Variable Viscosity on Theentropy Generation and Pumping Power in a Laminar Fluid Flow Through a Duct Subjected to Constant Heat Flux" Heat and MassTransfer 35 (1999): 499-506.

Salas, H., Cuevas, S., and M.L. de Haro. "Entropy Generation Analysis of Magnetohydrodynamic Induction Devices" Journal of Physics D: Applied Physics 32 (1999): 2605–8.

Thibault, J.P., Joussellin, F., Alemany, A., and A. Dupas. "The Possible Use of a Metal-Gas MHD Energy Converter in Space" Acta Astronautica 10 (1983): 587-9.

Tripathi, D., Anwar Bég, O., and J. Curiel-Sosa. "Homotopy Semi-Numerical Simulation of Peristaltic Flow of Generalised Oldroyd-B Fluids with Slip Effects" Computer Methods in Biomechanics and Biomedical Engineering (2012): DOI:10.1080/10255842.2012.688109.

Turkyilmazoglu, M., MHD Fluid Flow and Heat Transfer

due to a Stretching Rotating Disk, International Journal of Thermal Sciences 51 (2012): 195-201.

Von Kármán, T. "Über läminare und turbulence Reibung" ZAMM 1 (1921): 233-52.

Yamasaki, H., Kabashima, S., Shioda, S., and Y. Okuno. "Unsteady Discharge and Fluid Flow in a Closed-Cycle Disk MHD Generator" Journal of Propulsion and Power 4 (1988): 61-7.

Zhou, J.K. Differential Transformation and Its Applications for Electrical Circuits, Huazhong University Press, Wuhan, China, 1986.

Zueco, J., and O. Anwar Bég. "Network Numerical Analysis of Hydromagnetic Squeeze Film Flow Dynamics Between Two Parallel Rotating Disks with Induced Magnetic Field Effects" Tribology International 43 (2010): 532-43.

Zueco, J., Eguía, P., Granada, E., Míguez, J.L., and O. Anwar Bég. "An Electrical Network for the Numerical Solution of Transient MHD Couette Flow of a Dusty Fluid: Effects of Variable Properties and Hall Current" International Communications in Heat and Mass Transfer 37 (2010): 1432–9.